Inhibition of *MYC* suppresses programmed cell death ligand-1 expression and enhances immunotherapy in triple-negative breast cancer

Xintong Li[1], Lin Tang[2], Qin Chen[1], Xumin Cheng[3], Yiqiu Liu[1], Cenzhu Wang[1], Chengjun Zhu[1], Kun Xu[1], Fangyan Gao[1], Jinyi Huang[1], Runtian Wang[1], Xiaoxiang Guan[1,4]

[1]Department of Oncology, The First Affiliated Hospital of Nanjing Medical University, Nanjing, Jiangsu 210029, China;
[2]Medical School of Nanjing University, Nanjing, Jiangsu 210093, China;
[3]Department of Breast Surgery, The First Affiliated Hospital with Nanjing Medical University, Nanjing, Jiangsu 210029, China;
[4]Jiangsu Key Lab of Cancer Biomarkers, Prevention and Treatment, Collaborative Innovation Center for Personalized Cancer Medicine, Nanjing Medical University, Nanjing, Jiangsu 210029, China.

Abstract

Background: Cancer immunotherapy has emerged as a promising strategy against triple-negative breast cancer (TNBC). One of the immunosuppressive pathways involves programmed cell death-1 (PD-1) and programmed cell death ligand-1 (PD-L1), but many patients derived little benefit from PD-1/PD-L1 checkpoint blockades treatment. Prior research has shown that *MYC*, a master transcription amplifier highly expressed in TNBC cells, can regulate the tumor immune microenvironment and constrain the efficacy of immunotherapy. This study aims to investigate the regulatory relationship between *MYC* and PD-L1, and whether a cyclin-dependent kinase (CDK) inhibitor that inhibits *MYC* expression in combination with anti-PD-L1 antibodies can enhance the response to immunotherapy.

Methods: Public databases and TNBC tissue microarrays were used to study the correlation between *MYC* and PD-L1. The expression of *MYC* and PD-L1 in TNBCs was examined by quantitative real-time polymerase chain reaction and Western blotting. A patient-derived tumor xenograft (PDTX) model was used to evaluate the influence of a CDK7 inhibitor THZ1 on PD-L1 expression. Cell proliferation and migration were detected by 5-ethynyl-2′-deoxyuridine (EdU) cell proliferation and cell migration assays. Tumor xenograft models were established for *in vivo* verification.

Results: A high *MYC* expression level was associated with a poor prognosis and could alter the proportion of tumor-infiltrating immune cells (TIICs). The positive correlation between *MYC* and PD-L1 was confirmed by immunostaining samples from 165 TNBC patients. Suppression of *MYC* in TNBC caused a reduction in the levels of both PD-L1 messenger RNA and protein. In addition, antitumor immune response was enhanced in the TNBC cancer xenograft mouse model with suppression of *MYC* by CDK7 inhibitor THZ1.

Conclusions: The combined therapy of CDK7 inhibitor THZ1 and anti-PD-L1 antibody appeared to have a synergistic effect, which might offer new insight for enhancing immunotherapy in TNBC.

Keywords: Triple negative breast neoplasms; *MYC*; Programmed cell death ligand 1; PD-L1; CDK7; THZ1; Immunotherapy

Introduction

Triple-negative breast cancer (TNBC) is a molecularly heterogeneous subtype of breast cancer, clinicopathologically characterized by lack of estrogen and progesterone receptors, and human epidermal growth factor receptor 2 (HER2) overexpression.[1-3] It is a highly aggressive malignancy that comprises approximately 15% of all breast cancers, with a high recurrence rate, and a poor clinical prognosis.[4-7] Although the pathological studies of breast cancer are improving constantly, the clinical treatment effect of TNBC remains unsatisfactory.[8-10] Recently, immunotherapy has become available and approved for advanced TNBC. Therefore, considerable interest has been developed to elucidate the biologic mechanisms driving TNBC.

Of TNBCs, approximately 70% are molecularly categorized as basal-like, and further subdivided as either "inflamed" or "non-inflamed" according to their respec-

Access this article online

Quick Response Code:

Website: www.cmj.org

DOI: 10.1097/CM9.0000000000002329

Xintong Li and Lin Tang contributed equally to this work.

Correspondence to: Xiaoxiang Guan, Department of Oncology, The First Affiliated Hospital of Nanjing Medical University, 300 Guangzhou Road, Nanjing, Jiangsu 210029, China
E-Mail: xguan@njmu.edu.cn

Chinese Medical Journal 2022;135(20)

Received: 16-06-2022; **Online:** 09-12-2022 **Edited by:** Xiuyuan Hao and Rongman Jia

tive tumor immune microenvironment (TIME) phenotypes. Successful development of immune checkpoint inhibitors has shown a therapeutic benefit in increasing local antitumor immune response. The programmed cell death-1 (PD-1) /programmed cell death ligand-1 (PD-L1) axis is a major checkpoint pathway for immune responses within the tumor microenvironment. Several studies have investigated PD-L1 expression in clinical trials using monoclonal antibodies (mAbs) directed against the PD-1/PD-L1 pathway in breast cancer.[11] However, in TNBC patients, the response rate was lower than that observed in atezolizumab and pembrolizumab studies in other patients with different breast cancer subtypes who had PD-L1 positive tumors. Anti-PD-1/PD-L1 antibodies used as a single agent were able to induce a significant level of antitumor activity in only about 20% of TNBC patients, and only when tumor PD-L1 was expressed.[12] A deeper understanding of the means to improve the immunologic response of TNBC requires urgent investigation.

MYC is an overexpressed and aberrantly activated master transcription amplifier in tumors, which has been confirmed to play an imperative role in the tumorigenesis of a variety of tumors.[13,14] Numerous studies have confirmed that *MYC* is highly expressed in TNBC and closely associated with its poor prognosis.[15,16] Therapies targeting *MYC* have increasingly received intense attention in emerging cancer treatments. Many studies have found that the activation of *MYC* can stimulate the expression of PD-L1 that leads to tumor immune escape.[17,18] This suggests that inhibiting the expression of *MYC* in TNBC might enhance the effect of immunotherapy. For example, a cyclin-dependent kinase 7 (CDK7) inhibitor THZ1 has been shown to suppress the expression of *MYC*, which in turn reduces the expression of super-enhancer related genes and inhibits the growth of various cancers.[19-23] In the present study, the aims consisted of investigating: (1) the regulatory relationship between *MYC* and PD-L1; and (2) whether a CDK inhibitor that inhibits *MYC* expression in combination with anti-PD-L1 antibodies could enhance the response to immunotherapy.

Bioinformatics analysis and tissue microarrays of TNBC patients were used to investigate the correlation between the expression of *MYC* and PD-L1. THZ1 was utilized to inactivate MYC to determine whether PD-L1 expression was reduced in TNBC. Furthermore, the therapeutic combination of the CDK7 inhibitor THZ1 and anti-PD-L1 antibodies was utilized to determine its value as an immunotherapy agent in TNBC [Figure 1].

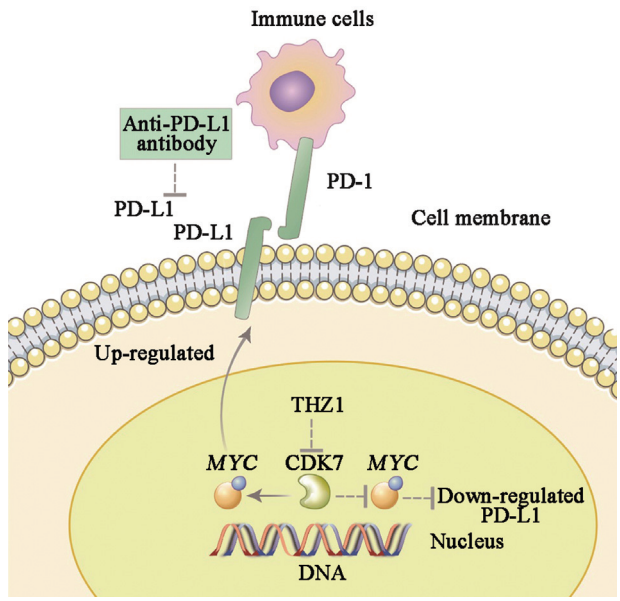

Figure 1: Inhibition of *MYC* by THZ1 suppresses PD-L1 expression and enhances antitumor immune response. CDK7: Cyclin-dependent kinase 7; PD-1: Programmed cell death-1; PD-L1: Programmed cell death ligand-1.

Methods

Public database and bioinformatics analysis

The GSE9893 database was extracted and analyzed to assess the association between *MYC* messenger RNA (mRNA) and prognosis of breast cancer. We used the CIBERSORT (http://cibersort.stanford.edu/) dataset to evaluate the interrelation between the immune response of 21 tumor-infiltrating immune cells (TIICs) and *MYC* expression in breast cancer, as well as the interrelations between TIICs.[24] The Cancer Genome Atlas (TCGA) (https://cancergenome.nih.gov/) dataset was applied to explore the correlation between *MYC* and T cell immunoreceptor with immunoglobulin and immunoreceptor tyrosine-based inhibition motif (ITIM) domain (TIGIT), cytotoxic T lymphocyte antigen-4 (CTLA-4), PD-L1, or lymphocyte-activation gene 3 (LAG3) expression levels of breast cancer.[25]

Tissue microarrays and immunohistochemistry

The tissue microarrays (HBreD075Bc01 and HBreD090Bc01), which contained TNBC samples from 165 breast cancer patients, were obtained from Outdo Biotech company (Shanghai, China). Anti-PD-L1 antibody (clone SP263, rabbit, Ventana, Arizona, USA) and anti-*MYC* antibody (ab39688) were used to perform immunohistochemistry staining. We characterized a positive PD-L1 expression as any membranous staining of ≥1% of tumor cells or immune cells. Furthermore, we categorized the degree of tumor staining as follows: A score of 0 indicated <1%, while 1, 2, and 3 indicated 1% to 5%, 6% to 50%, and >50%, respectively. A score of 1–3 was considered positive, and 0 indicated negative.[26,27] The intensities of *MYC* expression scores were assigned as follows: 0 (negative), 1 (weak), 2 (moderate), and 3 (strong). The percentages of positive cells scores were assigned as follows: 0 (≤5%), 1 (6–25%), 2 (26–50%), 3 (51–75%), and 4 (76–100%). We combined the two parameters into a total score. Two pathologists examined the immunohistochemical staining in a blinded manner. The cut-off value was 6 for *MYC*.[28] The patients were informed and consented for the study.

Cell lines and transfection assay

MCF-7, BT-474, BT-20, MDA-MB-231, BT-549, MB-157, and 4T1 cell lines were purchased from Chinese

Academy of Science Committee Type Culture Collection Cell Bank (Shanghai, China). These cell lines were cultured in Roswell Park Memorial Institute (RPMI) 1640 medium (Gibco, California, USA) supplemented with 10% fetal bovine serum (FBS) (ExCellBio, Shanghai, China), 100 U/mL penicillin (Gibco), and 100 U/mL streptomycin (Gibco) at 37°C with 5% CO_2 under fully humidified conditions. Small interfering RNA (siRNA) targeting *MYC* and an *MYC* overexpression plasmid pcDNA3.1-MYC were designed and synthesized in RiboBio Co., Ltd. (Guangzhou, China). The negative siRNA and empty plasmids were used as control. Cells were transfected with plasmids and siRNAs by using the Lipofectamine 3000 reagent (Invitrogen, Carlsbad, CA, USA) in accordance with the manufacturer's protocol. The *MYC*-targeted siRNAs sequences were as follows: siRNA-1: GAGGAGACATGGTGAACCA; siRNA-2: GG GTCAAGTTGGACAGTGT; siRNA-3: CGACGAGAC CTTCATCAAA.

Western blotting

Cells were harvested following THZ1 treatment for 48 h, and the total protein was extracted using a Radio Immunoprecipitation Assay lysis buffer (RIPA Sigma–Aldrich) containing the protease and the phosphatase inhibitor cocktails. The protein concentrations were quantified by using a bicinchoninic acid (BCA) kit (Beyotime, Shanghai, China). Western blotting analyses for PD-L1 and *MYC* were performed following the conventional protocols as described previously.[27] The analysis of bands was performed with the Image J software program (National Institutes of Health, Bethesda, Maryland, USA). The target proteins were incubated with the following antibodies: PD-L1 (Abcam, Cambridge, MA, USA; ab213524), MYC (Abcam, ab39688), Ki-67 (Cell Signaling Technology, #9449), and glyceraldehyde-3-phosphate dehydrogenase (GAPDH) (Abcam, ab181603). Antibodies were diluted according to manufacturer's recommendations. The CDK7 inhibitor THZ1 (HY-80013, MedChem Express, New Jersey, USA) was dissolved in dimethyl sulfoxide (DMSO).

Quantitative real-time polymerase chain reaction (PCR)

Total RNA was extracted from cells using TRIzol (Invitrogen). The quantitative PCR (qPCR) was performed with SYBR Green PCR Master Mix (Life Technology, New York, NY, USA), and gene-specific primers were as follows: PD-L1 gene (forward: 5′-GCTGCACTAATTGTCTATTGGGA-3′, reverse: 5′-AATTCGCTTGTAGTCGGCACC-3′), *MYC* gene (forward: 5′-TCCCTCCACTCGGAAGGAC-3′, reverse: 5′-CTGGTGCATTTTCGGTTGTTG-3′), and housekeeping gene *GAPDH* (forward: 5′-GGAGCGAGATC CCTCCAAAAT-3′, reverse: 5′-GGCTGTTGTCATACTTC TCATGG-3′). The relative expression of PD-L1 and *MYC* was determined with the $2^{-\Delta\Delta Ct}$ method by using the Step one plus Real time-PCR system (Applied Biosystems [ABI], Carlsbad, CA, USA).

Patient-derived tumor xenograft (PDTX)

Breast tumor tissues applied in the PDTX modeling were attained from surgical specimens of patients treated at The First Affiliated Hospital of Nanjing Medical University in August 2018. The Ethic Committee of the hospital approved the study (Nos. 2017NZGKJ-108, and 2019-SRFA-197), and we conducted the study under the guidance of the *Declaration of Helsinki*. The approaches for establishing PDTX were completed as previously illustrated.[29] The patients were informed and consented for the study.

5-ethynyl-2′-deoxyuridine (EdU) proliferation analysis

We investigated the proliferation of BT549 cells treated with THZ1, anti-PD-L1 antibody, and their combination using a Cell-Light EdU Cell Proliferation Kit (Abcam), according to the manufacturer's instructions. Briefly, the BT549 cells were seeded into the wells of a 24-well plate at a density of 2×10^5 per well. The cells of THZ1 (MedChem Express) and the combination groups were treated with 50 nmol/L THZ1 for 24 h. Anti-PD-L1 antibody (clone SP263, rabbit, Ventana) was added to fresh media at a final concentration of 10 μg/mL. After 1 h, the freshly isolated $CD8^+$ T cells were added to the media, and the ratio of $CD8^+$ T cells and BT549 cells was 5:1, and 24 h later, the medium was replaced with 100 μL of 10 μmol/L EdU medium in each well. The cells were then incubated for 2 h and fixed with 4% paraformaldehyde. They were permeated with 0.5% Triton X-100 for 10 min and were stained with iFluor 647 (Abcam) for 30 min. The cells were subsequently counterstained with 4′,6-diamidino-2-phenylindole (DAPI) and imaged via fluorescence microscopy (Olympus, Tokyo, Japan).

Cell migration assays

Cell migration assays were carried out by using 24-well transwell chambers with an 8 μm pore polycarbonate membrane insert (ThermoFisher Scientific, Waltham, Massachusetts, USA). For the THZ1 (MedChem Express) and combination group, the BT549 cells were pre-treated with 50 nmol/L THZ1 for 24 h, and then the cells were seeded at a density of 2×10^5 on the top side of the membrane without Matrigel. Later, 200 μL RPMI 1640 medium (Gibco) supplemented with 0.5% FBS (ExCell-Bio) was added to the upper chambers and 600 μL 10% FBS-1640 (ExCellBio) was added to the lower wells. Anti-PD-L1 antibody was added to the upper chambers at a final concentration of 10 μg/mL. After 1 h, the freshly isolated $CD8^+$ T cells were added to the upper chambers, and the ratio of $CD8^+$ T cells and BT549 cells was 5:1. The assays were carried out for 24 h at 37°C. Cells that migrated to the bottom of the upper membrane were collected mechanically and were fixed in 4% paraformaldehyde and stained with 0.05% crystal violet in methanol. Migration efficiency was determined by microscopy.

Tumor growth inhibition

Twenty Balb/c mice were injected with 2×10^6 4T1 cells in the right flank subcutaneous fat pad. After the tumor volume reached about 50 to 100 mm^3, the mice were randomly divided into four groups with five mice in each group, and were then injected intraperitoneally with THZ1 (10 mg/kg, twice a day) (MedChem Express), anti-PD-L1 antibody (250 μg, twice a week) (clone SP263,

rabbit, Ventana) a combination of THZ1 and anti-PD-L1 antibody, and saline, respectively. Tumor major diameter a and minor diameter b were measured, and the tumor volume was calculated using the formula $\pi/6 \times a \times b^2$. All animal experiments were approved by the Ethic Committee of the First Affiliated Hospital of Nanjing Medical University (No. 2019-SRFA-244).

Statistical analysis

SPSS 23.0 software (IBM, New York, USA) and GraphPad Prism Version 7 (GraphPad Software, San Diego, USA) were used to analyze the data and plot curves. We calculated the statistical significance with one-way analysis of variance (ANOVA) and Student's t-test. P values <0.05 were defined as statistically significant.

Results

Expression of MYC was associated with prognosis and TIICs in breast cancer patients

By using the GSE9893 database, we assessed the association between *MYC* gene expression and prognosis in breast cancer patients. The Kaplan–Meier analysis demonstrated that high *MYC* expression was significantly correlated with poor overall survival [Figure 2A]. Previous analyses suggested that the number and activity of tumor (i.e., infiltrating lymphocytes) had an influence on the clinical outcome of cancer patients.[30] In the present study, the CIBERSORT algorithm was used to estimate the landscape of tumor microenvironment immune infiltration under different degrees of *MYC* expression, and the correlation matrix revealed that the portions of different TIICs subpopulations had weak to moderate interplay with *MYC* in breast cancer [Figure 2B]. Macrophages M0 had a noteworthy negative correlation with the resting CD4 memory T cells (coefficient of relationship [Cor]=–0.52), $CD8^+$ T cells (Cor=–0.53), and naive B cells (Cor=–0.04). In contrast, M1 macrophages and resting CD4 memory T cells were most positively correlated in breast cancer samples (Cor=0.03). Additionally, we attempted to explore the interplay between *MYC* expression and infiltration level of 21 immune cells. As shown in Figure 2C, naive B cells, $CD8^+$ T cells, follicular helper T cells, regulatory T cells, M2 macrophages, and resting mast cells are the principal immune cells affected by *MYC* expression; specifically, compared with the low expression group, M2 macrophages ($P < 0.001$) and the resting mast cells ($P < 0.001$) shared a higher proportion in the high

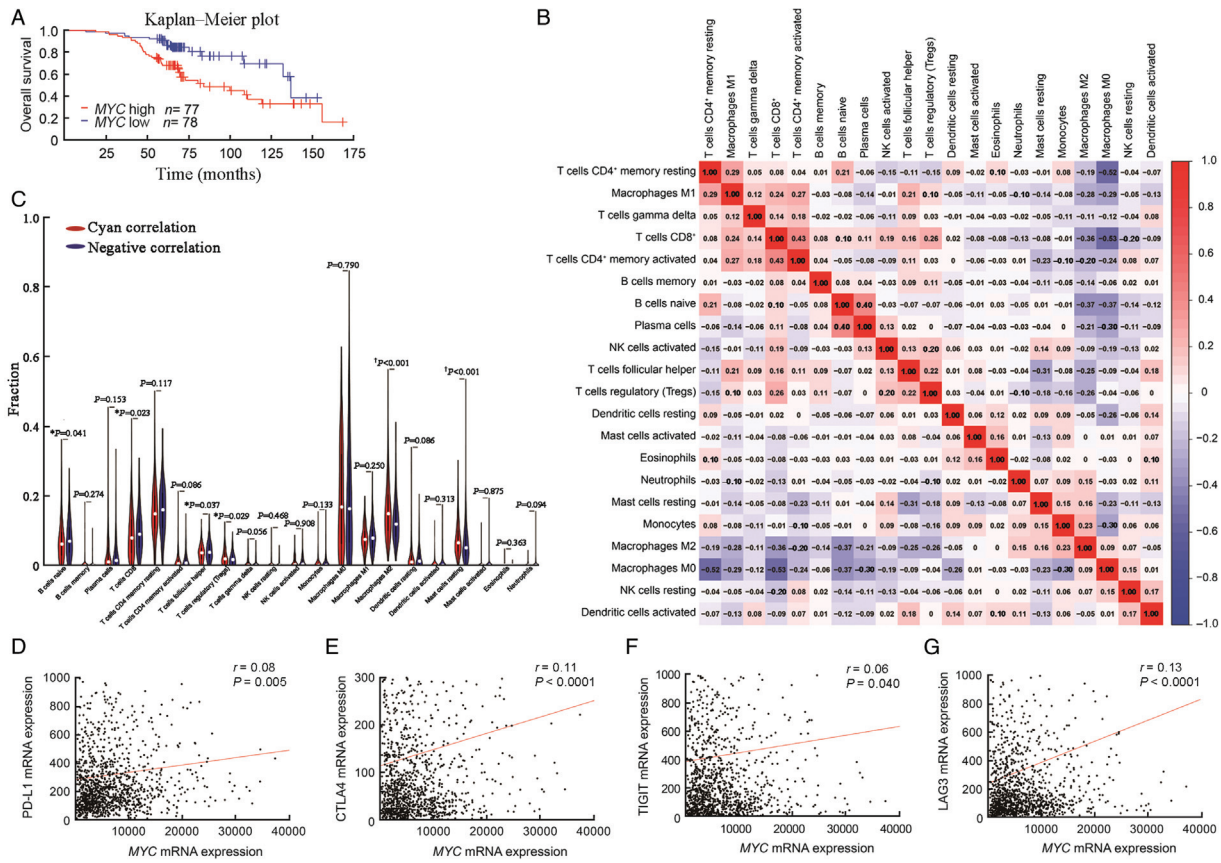

Figure 2: *MYC* expression was related to prognosis and TIICs in breast cancer patients. (A) Relationship between mRNA level of *MYC* and overall survival in the TCGA database (cut-off value: median, 0.5; $P = 0.047$). (B) Correlation heat map of 21 types of immune cells. The size of the colored squares represents the strength of the correlation; positive correlation was shown in cyan, and negative correlation was shown in red. The darker the color, the stronger the correlation was. (C) The proportion of 21 subpopulations of immune cells affected by *MYC* expression. Relationship between *MYC* and PD-L1 (D), CTLA-4 (E), TIGIT (F), and LAG3 (G) expressions in breast cancer cases from the TCGA database. $^*P < 0.05$; $^\dagger P < 0.001$. CTLA-4: Cytotoxic T lymphocyte antigen-4; LAG3: Lymphocyte-activation gene3; mRNA: Messenger ribonucleic acid; NK: Natural killer; PD-L1: Programmed cell death ligand-1; TCGA: The Cancer Genome Atlas; TIGIT: T cell immunoreceptor with immunoglobulin and immunoreceptor tyrosine-based inhibition motif (ITIM) domain; TIICs: Tumor-infiltrating immune cells.

expression group. In contrast, the portions of naive B cells ($P = 0.041$), CD8$^+$ T cells ($P = 0.023$), follicular helper T cells ($P = 0.037$), and regulatory T cells ($P = 0.029$) were notably lower. Consequently, we explored the potential influence of *MYC* expression on cancer immunotherapy and discovered an interaction between *MYC* and immune checkpoints expression, including PD-L1, CTLA-4, TIGIT, and LAG3 [Figures 2D–2G].

Expression of MYC was positively correlated with PD-L1 expression in TNBC

Immune checkpoint blockade therapy targeting the PD-1/PD-L1 axis reveals promising clinical effects in TNBC,[31] and a higher PD-L1 expression indicates a higher immune response. We evaluated the correlation between the expression of *MYC* and PD-L1 in human luminal breast cancer cell line MCF-7, HER2 overexpression breast cancer cell line BT-474, and TNBC lines BT-20, HCC1937, BT-549, MDA-MB-157, and MDA-MB-231. Among the seven breast cancer cell lines tested, HER2 overexpression breast cancer cell line BT-474 and two TNBC cell lines (BT-549 and MDA-MB-231) showed distinct *MYC* and PD-L1 expression levels, MDA-MB-157 cell line showed a weak expression, and the others showed no expression [Figures 3A and 3B]. In order to understand whether the expression of PD-L1 was related to the *MYC* expression level in TNBC patients, we used 165 tumor specimens of TNBC patients, stained them with anti-PD-L1 and anti-*MYC* antibodies, and assessed PD-L1 expression in both tumor cells and immune cells [Figure 3C]. The clinicopathological characteristics of TNBC are presented in Table 1. We found that the expression of PD-L1 was positively associated with high histological grade ($P = 0.004$), but not with age, T-stage, and N-status. We also found that 43.6% (72/165) of tumors expressed PD-L1 and 67.9% (112/165) of tumors expressed MYC [Table 2]. Next, statistical analysis of the immunohistochemistry (IHC) scores revealed that the PD-L1 protein levels of patients with the high expression of *MYC* were higher than those with the low *MYC* expression [Figures 3D and 3E]. Clearly, the expression levels of *MYC* and PD-L1 in TNBC tissues were positively correlated at the protein level.

MYC regulated PD-L1 expression in TNBC

Recent studies have indicated that *MYC* could regulate PD-L1 expression in some tumors.[19,20,32,33] To further

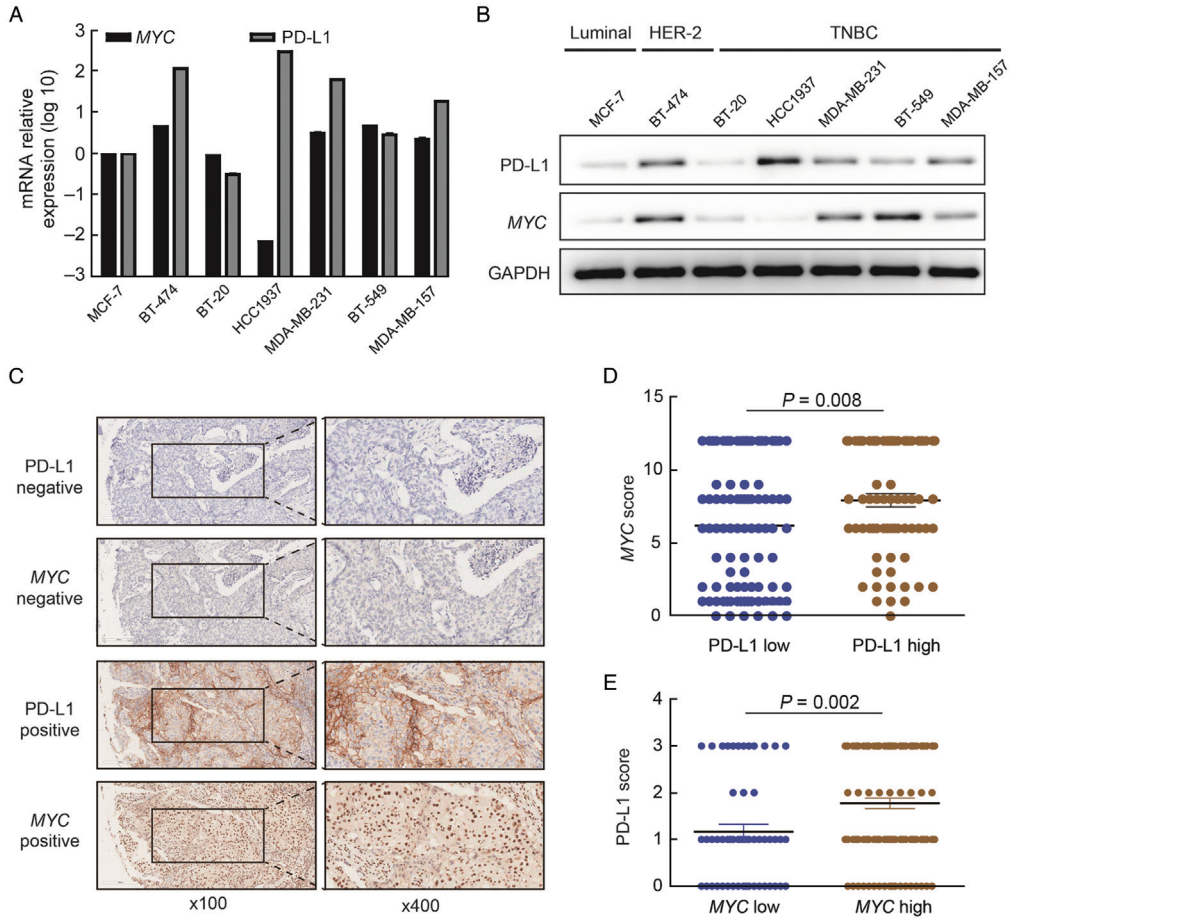

Figure 3: The expression of *MYC* was correlated with PD-L1 in TNBC patients. (A) RT-PCR and (B) Western blotting were performed to evaluate the expression levels of *MYC* and PD-L1 in breast cancer cell lines. (C) Immunohistochemical staining of *MYC* and PD-L1 in tumor specimens from TNBC patients. Representative photographs were taken at low (100×) and high magnification (400×). (D and E) The protein levels of PD-L1 and *MYC* were compared via statistical analysis on IHC scores between the low and high protein expression of PD-L1 or *MYC*, respectively. Error bars indicate standard error of the mean (SEM). GAPDH: Glyceraldehyde-3-phosphate dehydrogenase; HER2: Human epidermal growth factor receptor 2; IHC: Immunohistochemistry; MCF-7: Michigan Cancer Foundation-7; mRNA: Messenger ribonucleic acid; PD-L1: Programmed cell death ligand-1; RT-PCR: Reverse transcription-polymerase chain reaction; TNBC: Triple-negative breast cancer.

Table 1: Relationship between PD-L1 expression and clinicopathologic characteristics of triple-negative breast cancer samples ($n = 165$).

Variables	PD-L1		Total	*P*-value
	Low ($n = 93$)	High ($n = 72$)		
Age				0.535
<53 years	46	36	82	
≥53 years	47	36	83	
Pathology grade				0.004
Grade 1	6	1	7	
Grade 2	59	32	91	
Grade 3	28	39	67	
T stage				0.076
1	42	23	65	
2	46	43	89	
3	0	4	4	
4	2	1	3	
NA	3	1	4	
Nodal status				0.312
0	37	34	71	
1	12	12	24	
2	2	4	6	
3	6	2	8	
NA	36	20	56	
AJCC TNM				0.262
I	22	13	35	
II	26	30	56	
III	9	8	17	
NA	36	21	57	

AJCC: American Joint Committee on Cancer; NA: Not applicable; PD-L1: Programmed cell death ligand-1; TNM: Tumor node metastasis.

explore the regulatory relationship between *MYC* and PD-L1 in TNBC cells, we performed MYC inactivation and activation experiments. We designed three siRNA (#1, #2, and #3) targeting *MYC* and one *MYC* overexpression plasmid (pcDNA3.1-MYC); the mRNA levels of *MYC* and PD-L1 in the transfected cells were determined by reverse transcription-polymerase chain reaction (RT-PCR). When transfected with *MYC* siRNA, the mRNA level of *MYC* was significantly decreased in BT549 and MDA-MB-231 cells that originally overexpressed *MYC*. Moreover, following transfection of an *MYC*-overexpressing plasmid (pcDNA3.1-MYC) into BT20 cells, the mRNA levels of *MYC* and PD-L1 were significantly upregulated, compared with an empty vector plasmid [Figures 4A–4D]. Furthermore, *MYC* siRNA #3 was transfected into BT549 and MDA-MB-231 cell lines for 48 h, the protein levels of PD-L1 cell lines were determined by Western blotting [Figures 4E and 4F], and importantly, MYC inactivation resulted in rapid down-regulation of PD-L1 at both the mRNA and protein levels. In addition, MYC activation was significantly correlated with the expression of PD-L1 in BT-20 cells [Figure 4G]. These results demonstrated that *MYC* regulated PD-L1 expression in multiple human breast tumor types.

THZ1 regulated MYC-induced PD-L1 expression

It has also showed in a previous study that CDK7 inhibitor THZ1 suppresses *MYC* expression.[25] To further explore whether THZ1 could indirectly inhibit the expression of PD-L1, we treated BT549 and MDA-MB-231 cell lines with different concentrations (0, 50, and 100 nmol/L) of THZ1 for 48 h. We found that THZ1-suppressed *MYC* function resulted in a decreased expression of the mRNA and protein of PD-L1 as measured by qPCR and Western blotting, respectively [Figures 5A–5D]. Moreover, the reduction of mRNA and protein levels was THZ1 concentration-dependent.

Table 2: Correlation between the expression of *MYC* and PD-L1 in 165 tumor specimens of triple-negative breast cancer patients.

PD-L1 expression	MYC expression (*n*)				Pearson correlation	
	Positive	Negative	Total	Rate (%)	*r*	*P*-value
Positive	57	15	72	43.6	0.21	0.006
Negative	55	38	93	56.4		
Total	112	53	165	–		

PD-L1: Programmed cell death ligand-1; –: Not available.

Next, we explored the influences of THZ1 on PD-L1 expression in a TNBC PDTX model. The PDTX was obtained from a TNBC patient, and had a high expression level of *MYC*. The breast carcinoma tissue blocks were implanted subcutaneously into the triple-immunodeficient NOD/ShiltJ-*Prkdc* em26Cd52 *Il2rg* em26Cd22 (NCG) mice (female, 6–8 weeks old). At 3 to 5 days after inoculation, PDTX model mice were intraperitoneally injected with THZ1 (10 mg/kg, twice a day) for 7 days. After administration, the tumors were stripped from the mice, and the tissues were collected to test PD-L1, MYC, and Ki-67 levels via immunostaining. As shown in Figure 5E, immunohistochemical data demonstrated that THZ1 greatly reduced the expressions of *MYC* and PD-L1. In addition, the proliferation marker Ki-67 in the THZ1 treatment group was also markedly reduced.

THZ1 and anti-PD-L1 antibody possess a synergistic effect and enhance TNBC response to immunotherapy

Cell proliferation and migration have been key mechanisms of malignant cells and vital for an immune response. Therefore, we investigated the proliferation and migration of BT549 cells treated with a single drug or a combination of THZ1 and anti-PD-L1 antibody. In the EdU proliferation assays, the number of EdU-labeled cells in the combined administration group was significantly lower than that in the single administration group [Figure 6A]. The migration ability of BT549 cells in the combined administration group was also decreased significantly compared with the single administration group [Figure 6B]. These indicated that the impact of the combined administration was increased on both cell proliferation and migration.

Lastly, the combined therapeutic efficacy of THZ1 and anti-PD-L1 antibody was evaluated *in vivo*. Twenty Balb/c mice were injected with 2×10^6 4T1 cells in the right flank subcutaneous fat pad. After the tumor volume reached approximately 50 to 100 mm^3, the mice were randomly

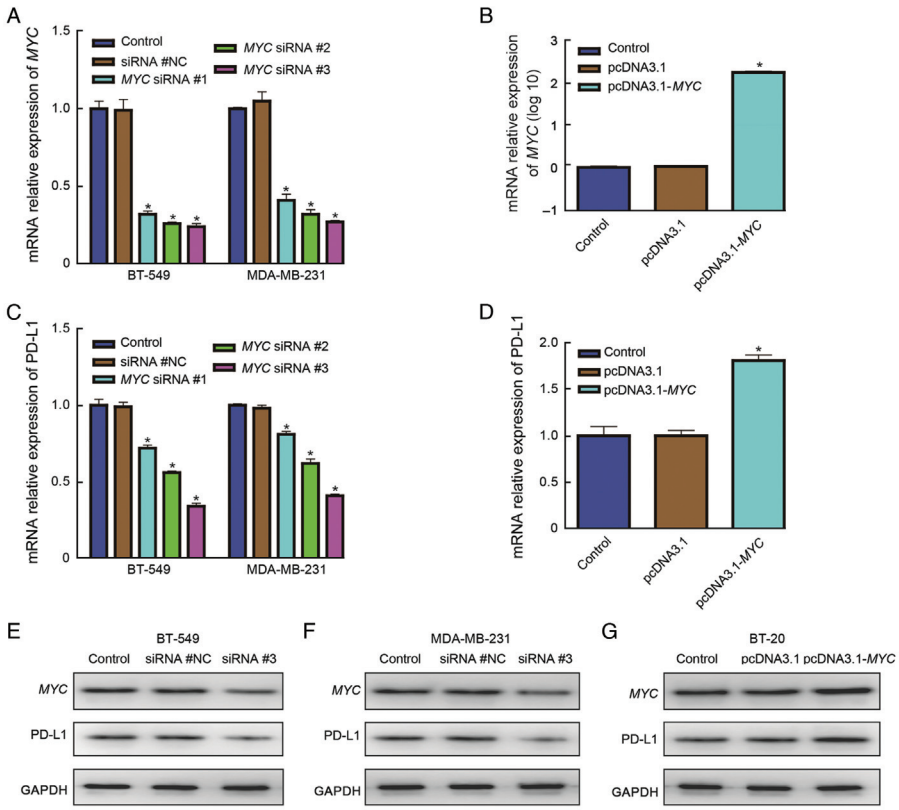

Figure 4: PD-L1 was regulated by *MYC* in TNBC cell lines. mRNA and protein levels of *MYC* and PD-L1 in human TNBC cell lines BT-549 (A, C, and E), MDA-MB-231 (A, C, and F) and BT-20 (B, D, and G) determined by qPCR and Western blotting, respectively, 48 h after MYC inactivation *in vitro*. MYC was inactivated by *MYC* siRNA knockdown. *MYC* was overexpressed by pcDNA3.1-MYC transfection ($n = 3$ biological and three technical replicates for qPCR). $^{*}P < 0.001$. Error bars indicate standard error of the mean (SEM). GAPDH: Glyceraldehyde-3-phosphate dehydrogenase; mRNA: Messenger ribonucleic acid; NC: Negative control; PD-L1: Programmed cell death ligand-1; qPCR: Quantitative polymerase chain reaction; siRNA: Small interfering RNA; TNBC: Triple-negative breast cancer.

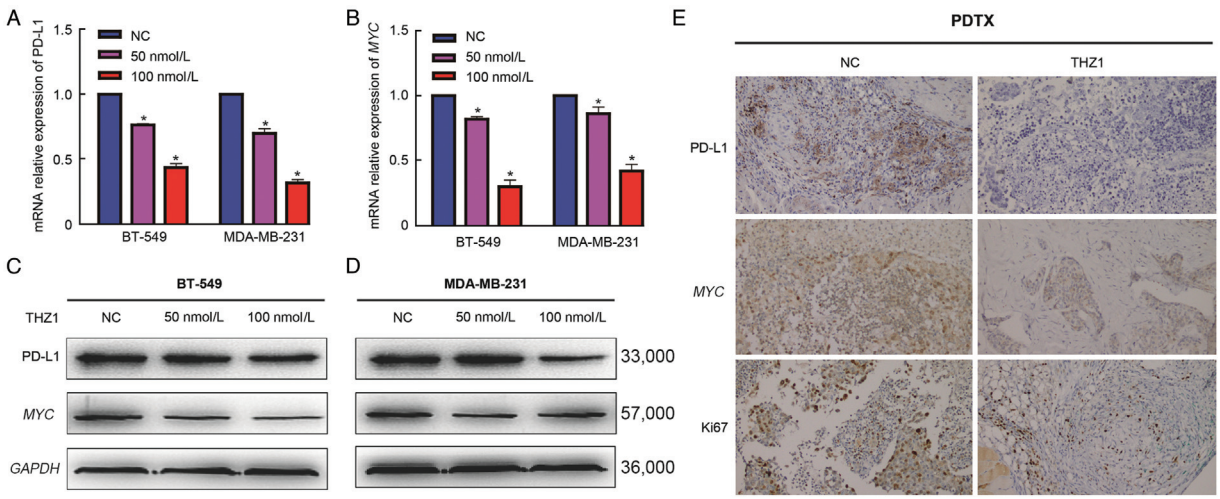

Figure 5: The expression of PD-L1 was suppressed by THZ1. mRNA (A and B) and protein (C and D) levels of PD-L1 and MYC in human TNBC cell lines BT-549 and MDA-MB-231 as determined by qPCR and Western blotting, respectively, 48 h after MYC inactivation *in vitro*. MYC was inactivated by different concentrations (50 nmol/L or 100 nmol/L) of THZ1 treatment ($n = 3$ biological and three technical replicates for qPCR). $^{*}P < 0.001$. Error bars indicate standard error of the mean (SEM). (E) Immunohistochemical staining of PD-L1, *MYC*, and Ki-67 in PDTX model of the patient (original magnification × 100). GAPDH: Glyceraldehyde-3-phosphate dehydrogenase; mRNA: Messenger ribonucleic acid; NC: Negative control; PD-L1: Programmed cell death ligand-1; PDTX: Patient-derived tumor xenograft; qPCR: Quantitative polymerase chain reaction; TNBC: Triple-negative breast cancer.

divided into four groups with five mice in each group and were then injected intraperitoneally with THZ1 (10 mg/kg, twice a day), anti-PD-L1 antibody (250 μg, twice a week), a combination of THZ1 and anti-PD-L1 antibody, and saline, respectively. As shown in Figure 6, the combined administration of THZ1 and anti-PD-L1 antibody showed improved inhibition of tumor growth than the single administration group. Taken together,

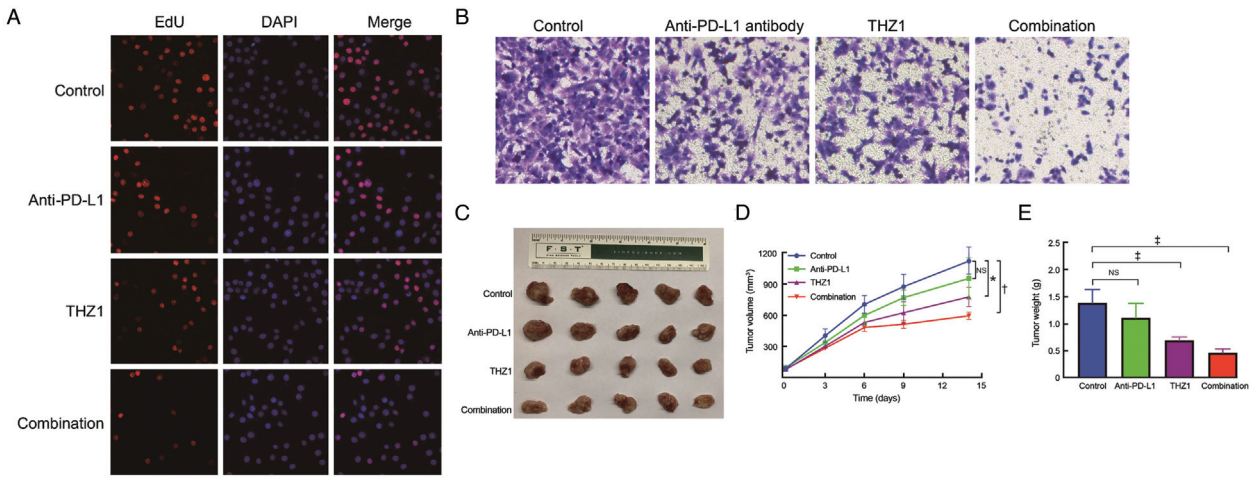

Figure 6: THZ1 and anti-PD-L1 antibody possess a synergistic effect on inhibiting tumor growth of triple-negative breast cancer. (A) Representative results of the EdU assay (original magnification: ×10). Dividing BT549 cells were labeled with EdU (red). All cells were counterstained with DAPI (blue). (B) The cell migration results after THZ1, anti-PD-L1 antibody, and combination of THZ1 and anti-PD-L1 antibody treatment (staining method: crystal violet dye; original magnification: ×10). Tumor growth inhibition in 4T1-tumor-bearing Balb/c mice injected with THZ1, anti-PD-L1 antibody, combination of THZ1 and anti-PD-L1 antibody, or saline intraperitoneally (five mice per group), respectively. Significant difference of the tumor volume (C and D) and tumor weight (E) between the combination and the saline groups was determined by Student's *t*-test ($^{*}P < 0.01$; $^{\dagger}P < 0.001$; $^{\ddagger}P < 0.05$). DAPI: 4′,6-diamidino-2-phenylindole; EdU: 5-ethynyl-2′-deoxyuridine; NS: Not significant; PD-L1: Programmed cell death ligand-1; TNBC: Triple-negative breast cancer.

these data suggest that THZ1 and anti-PD-L1 antibody have a synergistic effect and enhance TNBC response to immunotherapy *in vivo*.

Discussion

TNBC is the most aggressive breast cancer subtype, disproportionately affecting younger women, with high probability of distant metastasis and poor overall survival.[34-36] Because of the high level of immune infiltration in the primary tumor and immune gene expression signatures, TNBC was thought to have a high response to immunotherapy.[37,38] However, recent clinical trials have revealed that the overall response rate to pembrolizumab, a PD-1 mAb, was only 18.5% among the tested TNBC patients.[39] Thus, attention needs to be focused on those patients who can potentially achieve great benefits from PD-1/PD-L1 inhibitor monotherapy by identifying novel complementary biomarkers that facilitate enhanced targeted therapy.

Previous studies have shown that TIICs were the key regulators of anti-tumor immune response in the tumor microenvironment,[40] and were significantly associated with immune checkpoint suppression as well as clinical outcome.[30] We utilized TIICs as a research object to find biomarkers that might regulate the response to immunotherapy. The *MYC* proto-oncogene has been one of the most frequently activated oncogenes during tumorigenesis of various malignancies.[13,41] In the current study, we found that high expression of *MYC* was associated with a poor prognosis based on the GSE9893 database. We next focused on the association of *MYC* expression with immune infiltrating levels in breast cancer using the CIBERSORT analysis. The result revealed that the expression of *MYC* might have an important impact on TIICs composition and prognosis in breast cancer patients. Furthermore, prior reports have suggested that *MYC* overexpression is associated with a high expression of PD-L1 and promotes immune escape of tumor cells.[42] Nonetheless, the association between *MYC* and PD-L1 expression in TNBC remains uncertain. Therefore, we theorized that the *MYC*-regulated PD-L1 expression had a direct role in breast cancer, based on both the TCGA dataset and our patient data. Overexpression and depletion experiments further demonstrated that PD-L1 expression was regulated by *MYC* in breast cancer cell lines, consistent with previous studies.

Currently, the combination therapy of inhibitors of the predicted biomarkers and immune checkpoint blocking agent can improve efficacy and forestall the development of drug resistance among various cancer types.[42] Because some cancer types are especially sensitive to transcriptional inhibition, many small molecule inhibitors of CDK7, a protein kinase that directly regulates the activities of several transcription factors, have been developed.[23,43,44] THZ1 is one of the CDK7 inhibitors that has a strong inhibitory effect on TNBC cells. Logically, we chose THZ1 to investigate its role in the immune regulation of TNBC. Indeed, our data indicate that THZ1 inhibited the expression of *MYC* and PD-L1 in TNBC cell lines and PDTXs. Thus, we confirm that THZ1 suppresses *MYC*-regulated PD-L1 expression in TNBC. We also demonstrate that the combination therapy of THZ1 and anti-PD-L1 antibody even more effectively suppresses tumor growth in a TNBC xenograft mouse model.

In conclusion, our data show that the expression of PD-L1 positively correlate with and is regulated by the expression of *MYC* in TNBC cells. A small molecule CDK7 inhibitor THZ1, a drug that down-regulates the expression of *MYC*, can also effectively suppress PD-L1 expression. The mice immune response to anti-PD-L1 mAb was enhanced by an inactivated MYC system. We conclude that the combined therapy of THZ1 and anti-PD-L1 mAb may be

an effective treatment for TNBC, which provides a reference for clinical therapy.

Funding

This work was supported by the Key International Cooperation of the National Natural Science Foundation of China (No. 81920108029) and the Key Foundation for Social Development Project of the Jiangsu Province, China (No. BE2021741).

Conflicts of interest

None.

References

1. Wang YQ, Li HZ, Gong WW, Chen YY, Zhu C, Wang L, *et al*. Cancer incidence and mortality in Zhejiang Province, Southeast China, 2016: a population-based study. Chin Med J 2021;134:1959–1966. doi: 10.1097/CM9.0000000000001666.
2. Cao W, Chen HD, Yu YW, Li N, Chen WQ. Changing profiles of cancer burden worldwide and in China: a secondary analysis of the global cancer statistics 2020. Chin Med J 2021;134:783–791. doi: 10.1097/CM9.0000000000001474.
3. Denkert C, Liedtke C, Tutt A, von Minckwitz G. Molecular alterations in triple-negative breast cancer-the road to new treatment strategies. Lancet 2017;389:2430–2442. doi: 10.1016/S0140-6736(16)32454-0.
4. Collignon J, Lousberg L, Schroeder H, Jerusalem G. Triple-negative breast cancer: treatment challenges and solutions. Breast Cancer (Dove Med Press) 2016;8:93–107. doi: 10.2147/BCTT.S69488.
5. Bai YG, Gao GX, Zhang H, Zhang S, Liu YH, Duan XN, *et al*. Prognostic value of tumor-infiltrating lymphocyte subtypes in residual tumors of patients with triple-negative breast cancer after neoadjuvant chemotherapy. Chin Med J 2020;133:552–560. doi: 10.1097/CM9.0000000000000656.
6. Wang WY, Wang X, Liu JQ, Zhu Q, Wang X, Wang PL. Nomogram for predicting axillary lymph node pathological response in node-positive breast cancer patients after neoadjuvant chemotherapy. Chin Med J 2021;135:333–340. doi: 10.1097/CM9.0000000000001876.
7. Liu LP, Sun JH, Liu ZC. Mammographic density and risk of breast cancer recurrence and mortality. Chin Med J 2022. doi: 10.1097/CM9.0000000000001943.
8. Li LX, Zhang D, Liu BL, Lv D, Zhai JT, Guan XW, *et al*. Antibody-drug conjugates in HER2-positive breast cancer. Chin Med J 2021;135:261–267. doi: 10.1097/CM9.0000000000001932.
9. Lu ZN, Song J, Sun TH, Sun G. UBE2C affects breast cancer proliferation through the AKT/mTOR signaling pathway. Chin Med J 2021;134:2465–2474. doi: 10.1097/CM9.0000000000001708.
10. Luo CY, Li N, Lu B, Cai J, Lu M, Zhang YH, *et al*. Global and regional trends in incidence and mortality of female breast cancer and associated factors at national level in 2000 to 2019. Chin Med J 2021;135:42–51. doi: 10.1097/CM9.0000000000001814.
11. Zhao J, Huang J. Breast cancer immunology and immunotherapy: targeting the programmed cell death protein-1/programmed cell death protein ligand-1. Chin Med J 2020;133:853–862. doi: 10.1097/CM9.0000000000000710.
12. Schmid P, Adams S, Rugo HS, Schneeweiss A, Barrios CH, Iwata H, *et al*. Atezolizumab and Nab-Paclitaxel in advanced triple-negative breast cancer. N Engl J Med 2018;379:2108–2121. doi: 10.1056/NEJMoa1809615.
13. Dang CV. MYC on the path to cancer. Cell 2012;149:22–35. doi: 10.1016/j.cell.2012.03.003.
14. Walz S, Lorenzin F, Morton J, Wiese KE, von Eyss B, Herold S, *et al*. Activation and repression by oncogenic MYC shape tumour-specific gene expression profiles. Nature 2014;511:483–487. doi: 10.1038/nature13473.
15. Wang JK, Li M, Chen DL, Nie JY, Xi Y, Yang XJ, *et al*. Expression of C-myc and β-catenin and their correlation in triple negative breast cancer. Minerva Med 2017;108:513–517. doi: 10.23736/S0026-4806.17.05213-2.
16. Katsuta E, Yan L, Takeshita T, McDonald KA, Dasgupta S, Opyrchal M, *et al*. High MYC mRNA expression is more clinically relevant than MYC DNA amplification in triple-negative breast cancer. Int J Mol Sci 2019;21:217–228. doi: 10.3390/ijms21010217.
17. Casey SC, Baylot V, Felsher DW. The MYC oncogene is a global regulator of the immune response. Blood 2018;131:2007–2015. doi: 10.1182/blood-2017-11-742577.
18. de Jonge AV, Mutis T, Roemer MGM, Scheijen B, Chamuleau MED. Impact of MYC on anti-tumor immune responses in aggressive B cell non-hodgkin lymphomas: consequences for cancer immunotherapy. Cancers (Basel) 2020;12:3052–3072. doi: 10.3390/cancers12103052.
19. Pan Y, Fei QL, Xiong P, Yang JY, Zhang ZY, Lin XC, *et al*. Synergistic inhibition of pancreatic cancer with anti-PD-L1 and c-Myc inhibitor JQ1. Oncoimmunology 2019;8:e1581529. doi: 10.1080/2162402X.2019.1581529.
20. Casey SC, Tong L, Li YL, Do R, Walz S, Fitzgerald KN, *et al*. MYC regulates the antitumor immune response through CD47 and PD-L1. Science 2016;352:227–231. doi: 10.1126/science.aac9935.
21. Wang YB, Zhang TH, Kwiatkowski N, Abraham BJ, Lee TI, Xie SZ, *et al*. CDK7-dependent transcriptional addiction in triple-negative breast cancer. Cell 2015;163:174–186. doi: 10.1016/j.cell.2015.08.063.
22. Chipumuro E, Marco E, Christensen CL, Kwiatkowski N, Zhang TH, Hatheway CM, *et al*. CDK7 inhibition suppresses super-enhancer-linked oncogenic transcription in MYCN-driven cancer. Cell 2014;159:1126–1139. doi: 10.1016/j.cell.2014.10.024.
23. Christensen CL, Kwiatkowski N, Abraham BJ, Carretero J, Al-Shahrour F, Zhang TH, *et al*. Targeting transcriptional addictions in small cell lung cancer with a covalent CDK7 inhibitor. Cancer Cell 2014;26:909–922. doi: 10.1016/j.ccell.2014.10.019.
24. Newman AM, Liu CL, Green MR, Gentles AJ, Feng WG, Xu Y, *et al*. Robust enumeration of cell subsets from tissue expression profiles. Nat Methods 2015;12:453–457. doi: 10.1038/nmeth.3337.
25. Tang ZF, Li CW, Kang BX, Gao G, Li C, Zhang ZM. GEPIA: a web server for cancer and normal gene expression profiling and interactive analyses. Nucleic Acids Res 2017;45:W98–W102. doi: 10.1093/nar/gkx247.
26. Doğukan R, Uçak R, Doğukan FM, Tanık C, Çitgez B, Kabukcuoğlu F. Correlation between the expression of PD-L1 and clinicopathological parameters in triple negative breast cancer patients. Eur J Breast Health 2019;15:235–241. doi: 10.5152/ejbh.2019.4912.
27. Herbst RS, Soria JC, Kowanetz M, Fine GD, Hamid O, Gordon MS, *et al*. Predictive correlates of response to the anti-PD-L1 antibody MPDL3280A in cancer patients. Nature 2014;515:563–567. doi: 10.1038/nature14011.
28. Khan F, Ricks-Santi LJ, Zafar R, Kanaan Y, Naab T. Expression of p27 and c-Myc by immunohistochemistry in breast ductal cancers in African American women. Ann Diagn Pathol 2018;34:170–174. doi: 10.1016/j.anndiagpath.2018.03.013.
29. Liu Y, Zhu YP, Cai MZ, Ke B, Li B, Liu N, *et al*. A preliminary study on the establishment of the PDTX model. Cancer Manag Res 2020;12:1969–1979. doi: 10.2147/CMAR.S230668.
30. Azimi F, Scolyer RA, Rumcheva P, Moncrieff M, Murali R, McCarthy SW, *et al*. Tumor-infiltrating lymphocyte grade is an independent predictor of sentinel lymph node status and survival in patients with cutaneous melanoma. J Clin Oncol 2012;30:2678–2683. doi: 10.1200/JCO.2011.37.8539.
31. Zou JH, Zhuang MW, Yu XP, Li N, Mao RD, Wang ZD, *et al*. MYC inhibition increases PD-L1 expression induced by IFN -γ in hepatocellular carcinoma cells. Mol Immunol 2018;101:203–209. doi: 10.1016/j.molimm.2018.07.006.
32. Tang L, Jin J, Xu K, Wang X, Tang JH, Guan XX. SOX9 interacts with FOXC1 to activate MYC and regulate CDK7 inhibitor sensitivity in triple-negative breast cancer. Oncogenesis 2020;9:47–58. doi: 10.1038/s41389-020-0232-1.
33. Xia CF, Dong XS, Li H, Cao MM, Sun DQ, He SY, *et al*. Cancer statistics in China and United States, 2022: profiles, trends, and determinants. Chin Med J 2022;135:584–590. doi: 10.1097/CM9.0000000000002108.
34. Lyu MH, Ma YZ, Tian PQ, Guo HH, Wang C, Liu ZZ, *et al*. Development and validation of a nomogram for predicting survival of breast cancer patients with ipsilateral supraclavicular lymph node metastasis. Chin Med J 2021;134:2692–2699. doi: 10.1097/CM9.0000000000001755.

35. Tang P, Hu Y, Wang ZH, Gao GX, Qu X, Jiang J, *et al*. Clinical practice guidelines for endoscopic breast surgery in patients with early-stage breast cancer: Chinese Society of Breast Surgery (CSBrS) practice guidelines 2021. Chin Med J 2021;134:2532–2534. doi: 10.1097/CM9.0000000000001592.
36. Tomioka N, Azuma M, Ikarashi M, Yamamoto M, Sato M, Watanabe KI, *et al*. The therapeutic candidate for immune checkpoint inhibitors elucidated by the status of tumor-infiltrating lymphocytes (TILs) and programmed death ligand 1 (PD-L1) expression in triple negative breast cancer (TNBC). Breast Cancer 2018;25:34–42. doi: 10.1007/s12282-017-0781-0.
37. Zhuang XF, Shi GL, Hu X, Wang HR, Sun W, Wu YH. Interferon-gamma inhibits aldehyde dehydrogenasebright cancer stem cells in the 4T1 mouse model of breast cancer. Chin Med J 2021;135:194–204. doi: 10.1097/CM9.0000000000001558.
38. Nanda R, Chow LQ, Dees EC, Berger R, Gupta S, Geva R, *et al*. Pembrolizumab in patients with advanced triple-negative breast cancer: phase Ib KEYNOTE-012 study. J Clin Oncol 2016;34:2460–2467. doi: 10.1200/JCO.2015.64.8931.
39. Gajewski TF, Schreiber H, Fu YX. Innate and adaptive immune cells in the tumor microenvironment. Nat Immunol 2013;14:1014–1022. doi: 10.1038/ni.2703.
40. Beroukhim R, Mermel CH, Porter D, Wei G, Raychaudhuri S, Donovan J, *et al*. The landscape of somatic copy-number alteration across human cancers. Nature 2010;463:899–905. doi: 10.1038/nature08822.
41. Casey SC, Baylot V, Felsher DW. MYC: master regulator of immune privilege. Trends Immunol 2017;38:298–305. doi: 10.1016/j.it.2017.01.002.
42. Hu SH, Marineau JJ, Rajagopal N, Hamman KB, Choi YJ, Schmidt DR, *et al*. Discovery and characterization of SY-1365, a selective, covalent inhibitor of CDK7. Cancer Res 2019;79:3479–3491. doi: 10.1158/0008-5472.CAN-19-0119.
43. Patel H, Periyasamy M, Sava GP, Bondke A, Slafer BW, Kroll SHB, *et al*. ICEC0942, an orally bioavailable selective inhibitor of CDK7 for cancer treatment. Mol Cancer Ther 2018;17:1156–1166. doi: 10.1158/1535-7163.MCT-16-0847.
44. Wang BY, Liu QY, Cao J, Chen JW, Liu ZS. Selective CDK7 inhibition with BS-181 suppresses cell proliferation and induces cell cycle arrest and apoptosis in gastric cancer. Drug Des Devel Ther 2016;10:1181–1189. doi: 10.2147/DDDT.S86317.

How to cite this article: Li X, Tang L, Chen Q, Cheng X, Liu Y, Wang C, Zhu C, Xu K, Gao F, Huang J, Wang R, Guan X. Inhibition of *MYC* suppresses programmed cell death ligand-1 expression and enhances immunotherapy in triple-negative breast cancer. Chin Med J 2022;135:2436–2445. doi: 10.1097/CM9.0000000000002329